Theor Chim Acta (1995) 91: 179–186

Theoretica
Chimica Acta

Transition state localization by a density functional method. Applications to isomerization and symmetry-forbidden reactions

Yuri Abashkin, Nino Russo, Marirosa Toscano

Dipartimento di Chimica, Universita' della Calabria, I-87030 Arcavacata di Rende (CS), Italy

Received May 26, 1994/Final revision received August 9, 1994/Accepted August 11, 1994

Summary. A new transition state algorithm incorporated into the density functional code deMon, has been used to study the *trans* → *cis*-hydroxymethylene and *trans*-hydroxymethylene → formaldehyde isomerization processes and to localize the transition state for the decomposition of 1,3-diazacyclobutane to methyleneimine. Calculations have been performed using both local (LSD) and nonlocal spin density (NLSD) gradient-corrected approximations. Two different basis sets of small and large size have been used for the study in order to analyze the effect of the basis set dimension other than that of the nonlocal corrections on the activation energy barrier value. The results seem to confirm that density functional methods can be considered practical and reliable tools for the localization of transition states.

1. Introduction

Finding the critical points on a potential energy surface (PES) is a necessary step in the description of a chemical reaction. In contrast to locating minima, which is a fairly routine procedure in computational chemistry, transition state (TS) optimization is a much more difficult task. The application of standard Hartree–Fock methods for the location of transition states has a long tradition in quantum chemical computations. From this experience it is evident that the HF treatment, in which correlation is not taken into account, generally gives a poor description of potential energy surfaces and in particular in the prediction of reliable activation energy barriers. On the other hand, the introduction of correlation, more common in recent years because of increasingly more powerful computers, significantly increases the computational costs and can be used only for chemical systems of small or medium size. In this situation, density functional (DF) methods can provide a good (more practicable) alternative. It is well known that these methods give reliable predictions of many physical observables at relatively low computational cost. Furthermore, DF computer codes have recently been enhanced with the introduction of automatic TS search algorithms allowing saddle points or potential energy surfaces to be determined. For example, Fan and Ziegler [1, 2] have implemented the ADF [3] code, Stanton and Merz [4] have incorporated

Baker's transition state algorithm into the deMon package and very recently Abashkin and Russo [5] have proposed a new algorithm for TS localization, which has also been implemented in deMon [6]. This latter algorithm is based on a step-by-step walk uphill along the minimum energy path, allowing the automatic search and consequent refinement of saddle points. Previous studies [7] on some representative isomerization reaction have demonstrated that with this procedure reliable results at relatively low computational cost can be obtained.

In this paper we report a study of the different paths for HOCH isomerization and the potential energy profile for the decomposition of 1,3-diazocyclobutane. Many theoretical studies have been devoted to the former reaction, so it can be considered as a further good test for the proposed algorithm. The latter process is a symmetry-forbidden reaction and it is interesting both from fundamental and applied points of view.

2. Method

The strategic importance of the potential energy surface (PES) characterization of chemical reactions is well known. The most difficult work concerns the localization of transition state structures. In the last 20 years, different approaches have been proposed for a reliable and inexpensive search of saddle points on the PES [8–18].

Recently, we have developed and tested a new algorithm [5, 7] for TS location followed by a refining procedure. The background of our method is constrained optimization techniques. There are several features which make the algorithm attractive to use. It follows a minimum energy path (MEP). Such a reaction path is uniquely defined, does not depend on step size and has "chemical sense". The algorithm can be started from either the reactant or product geometry. Finally, the approach does not require the Hessian matrix and uses only first derivatives. Full details of the method can be found elsewhere [5]. In this paper we stress only the principal features of the algorithm.

According to the basic concept of the constrained optimization procedure [14], a new point lying on the MEP can be generated by minimizing the energy on a hypersphere, centered around some point (reactant geometry, for example) on the MEP.

One can choose a suitable strategy for changing the hypersphere radius and in such a way walk along the MEP for the reaction. As proposed in our previous paper [5], the constrained minimization is done in a straightforward manner. A standard minimization in $(n-1)$-dimensional space using analytical first derivatives can be used for finding the lowest energy on a hypersphere with some radius R. Thus, efficient quasi-Newton optimization techniques may be applied for solving the constrained optimization. The refining procedure includes an iterative process for moving along the reaction coordinate with energy relaxation in the remaining subspace. On the final step the Hessian matrix is calculated and analyzed to confirm that the stationary point found is indeed a transition state.

Vosko, Wilk and Nusair's parameterization of the correlation energy of the homogeneous electron gas has been used [19]. Nonlocal density corrections have has been included self-consistently using the functional of Perdew and Wang for exchange and that of Perdew [20] for correlation. Minimization in the constrained subspace has been performed by using the Broyden–Fletcher–Goldfarb–Shanno algorithm [21–24].

3. Result and discussion

3.1. Isomerization reactions

In the computations denoted SB (small basis), carbon and oxygen orbital basis sets (OBS) with a (521/41) contraction pattern have been used, while the hydrogen orbital basis has a (41/1) contraction pattern. The corresponding auxiliary basis set (ABS) used in the fitting of the charge density and the exchange-correlation potential are (5,2; 5,2) for C and O and (5,1; 5,1) for H atoms. In the case of the LB (large basis) calculation, the OBS are (7111/411/1*) for C and O with ABS of the form (4,4; 4,4). For the hydrogen atom the same OBS and ABS as for the small basis was used.

Starting from *trans*-hydroxymethylene (A in scheme 1), the *cis* form B can be reached by two different pathways that involve a motion of the hydrogen (H_1) atom in or out the molecular plane. We have located the transition states corresponding to these two different mechanisms (TS_1 and TS_2 of scheme 1). The formation of formaldehyde (C) arises from hydrogen (H_1) shift via the transition state (TS_3). The geometrical parameters of minima A, B and C are reported in Table 1 while those of the transition states are collected in Table 2. Energetic parameters for both the minima and transition states are reported in Table 3.

All the minima structures are planar and the geometrical parameters obtained at different levels of calculation are in good agreement with available experimental data [25] and previous high-level theoretical studies [4, 26–29]. The best agreement is obtained when the large basis set is used. Because the formaldehyde

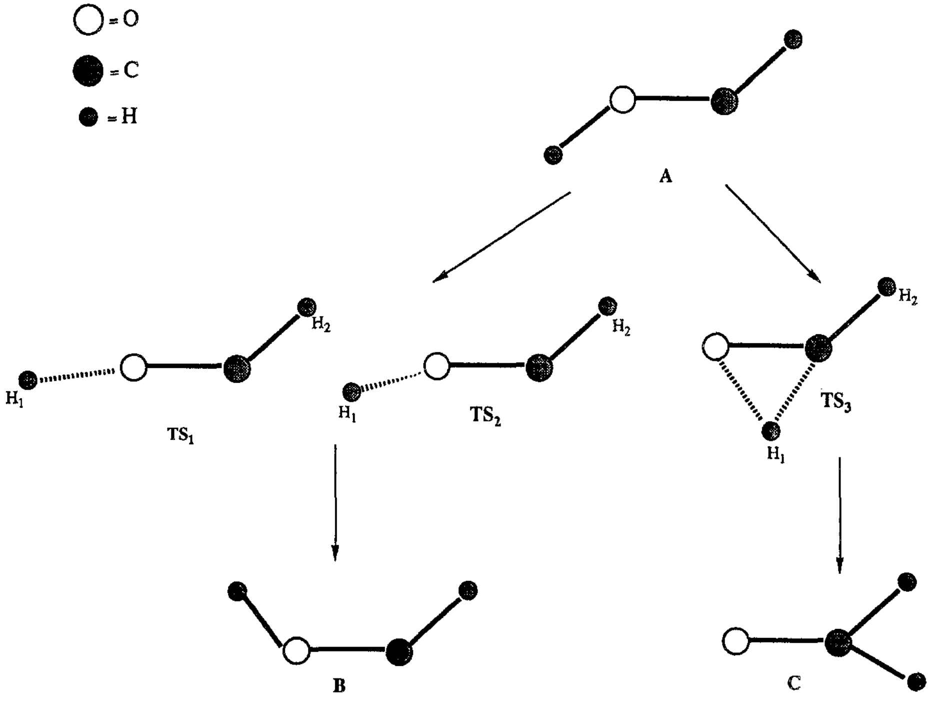

Scheme 1

Table 1. Geometrical parameters of minima in the isomerization reaction of HOCH. Distance are in Å, angles in degrees

Molecule	Method	R_{O-H}	R_{C-O}	R_{C-H}	HOC	OCH	HCH
A	LSD-SB	0.939	1.287	1.085	116.2	108.8	–
A	LSD-LB	0.983	1.309	1.131	108.4	101.6	–
A	NLSD-LB	0.982	1.333	1.128	108.3	101.5	–
B	LSD-SB	0.956	1.266	1.114	125.3	112.1	–
B	LSD-SB	0.994	1.301	1.135	117.3	107.1	–
B	NLSD-LB	0.993	1.324	1.138	116.8	106.8	–
C	LSD-SB	–	1.194	1.113	–	125.8	108.3
C	LSD-LB	–	1.206	1.121	–	121.9	116.2
C	NLSD-LB	–	1.216	1.116	–	121.7	116.6

Table 2. Geometrical parameters of transition states structures involved in the isomerization reactions of HOCH. Distance are in Å, angles in degrees

Molecule	Method	R_{O-H1}	R_{C-O}	R_{C-H1}	R_{C-H2}	H_1OC	OCH_2	H_1OCH_2
TS1	LSD-SB	0.925	1.276	–	1.121	175.7	108.1	0.0
	LSD-LB	0.964	1.305	–	1.145	177.8	103.1	0.0
	NLSD-LB	0.963	1.331	–	1.143	177.6	103.4	0.0
TS2	LSD-SB	–	–	–	–	–	–	–
	LSD-LB	0.975	1.341	–	1.152	125.6	103.9	92.1
	NLSD-LB	0.972	1.365	–	1.143	123.1	104.1	91.9
	NL-SCP[a]	0.969	1.353	–	1.142	121.3	104.9	90.1
	HF[b]	0.929	1.344	–	1.113	115.9	105.0	90.1
	MP2[b]	0.946	1.347	–	1.124	117.6	104.1	91.1
	LDA[b]	0.962	1.325	–	1.163	129.2	104.3	93.0
	NLDA[b]	0.973	1.358	–	1.160	120.3	104.1	92.1
TS3	LSD-SB	1.141	1.284	1.273	1.077	63.1	124.9	0.0
	LSD-LB	1.164	1.306	1.286	1.127	62.5	113.6	0.0
	NLSD-LB	1.173	1.325	1.286	1.124	61.6	113.4	0.0
	NL-SCF[a]	1.176	1.316	–	1.124	61.5	114.4	–
	HF[b]	–	1.270	1.097	1.171	59.2	116.2	–
	MP2[b]	–	1.322	1.106	1.154	60.5	113.2	–
	LDA[b]	–	1.207	1.135	1.166	61.8	113.7	–
	NLDA[b]	–	1.324	1.132	1.177	60.7	113.8	–

[a] from Ref. [2]
[b] from Ref. [4]

reaction has been extensively studied by a variety of different theoretical methods (HF [4], MP2 [4], MP4 [26, 27], CISD [28] and DF [4, 29]) a comparison of our transition state structures is possible.

TS1 and TS3 are planar at both the LSD and NLSD-LB levels. Using Baker's transition state locating algorithm in the deMon code, Stanton and Merz [4] find TS3 to be nonplanar. Unfortunately, these authors do not report their torsional angle, so further comparisons are not possible. In any case good agreement is found with their bond lengths and valence angles. The agreement is also good with other *ab initio* results. As a general feature we note that results obtained for both minima

Table 3. Relative stability of minima and transition states for the isomerization reactions of HOCH. Data are in kcal/mol

Molecule	LSD-SB	LSD-LB	NLSD-LB	NL-SCF[a]	NLDA[b]	HF[b]	MP2[b]	MP4[c]	CISD[d]
A	56.2	53.5	52.9	52.5	53.4	49.1	59.1	53.2	51.6
B	57.2	58.7	57.8	56.8	58.3	54.6	64.5	59.2	57.1
C	0.0	0.0	0.0	0.0	0.0	0.0	0.0	0.0	0.0
TS1	70.8	86.7	88.3	–	–	–	–	–	–
TS2	80.8	84.3	83.1	82.5	85.1	76.8	89.5	86.4	–
TS3	88.4	79.3	83.2	81.7	80.8	100.6	90.5	85.8	92.4

[a] from Ref. [2]
[b] from Ref. [4]
[c] from Refs. [26, 27]
[d] from Ref. [28]

and TS employing the small basis set give bond lengths that are shorter than those obtained with the large basis set using nonlocal corrections. Note that we were unable to locate TS2 with the small basis. Examination of Table 3 shows, as expected, that the most stable structure, in all cases is formaldehyde (C). In agreement with previous theoretical computations the trans form (A) is always more stable than the cis (B). The energy difference between these two minima ranges from 1 kcal/mol (at the SB level), to 5.2 kcal/mol (at the LB level) to 4.9 kcal/mol (at the NLSD-LB level). Our NLSD-LB results agree with the NLDA study of Stanton and Merz [4], in which the Becke exchange potential [30] was used, and with MP2 and MP4 values [4, 26, 27]. At NLSD-LB, *trans*-hydroxymethylene lies 52.9 kcal/mol above formaldehyde. Experimentally, the enthalpy difference between formaldehyde and *trans*-hydroxymethylene has been determined by ion cyclotron double resonance spectroscopy to be 54 kcal/mol [31]. An MP4 study [27] gives a value of 53.1 kcal/mol.

As previously mentioned, we have examined two possible mechanisms for the conversion of structure A to B. From table 3 it is evident that the mechanism that occurs via H1 out-of-plane rotation around the single O–C bond is slightly favoured with respect to the planar rearrangement. In fact, TS2 is 2.4 (LB) and 5.2 kcal/mol (NLSD-LB) lower than TS1. Our calculated barriers are somewhat lower than those obtained at MP2 and MP4 levels.

The isomerization A → C occurs via TS3 which lies 88.4, 79.3 and 82.2 kcal/mol above C at the SB, LB and NLSD-LB level, respectively. At the HF level the barrier is 100.6 kcal/mol; MP2 and MP4 studies [4, 26, 27] predict barriers of 90.5 and 85.8 kcal/mol, respectively.

Finally, we note that the potential energy reaction profile obtained using the Perdew and Wang and Perdew functional for nonlocal corrections is similar to that obtained employing the Perdew [20] and Becke functionals [30].

3.2. 1,3-diazacyclobutane decomposition

Because of their importance as "energetic molecules" the decomposition of nitramines has been the subject of several studies [32]. From a theoretical point of view the ring opening of 1,3-diazacyclobutane to methyleneimine is interesting

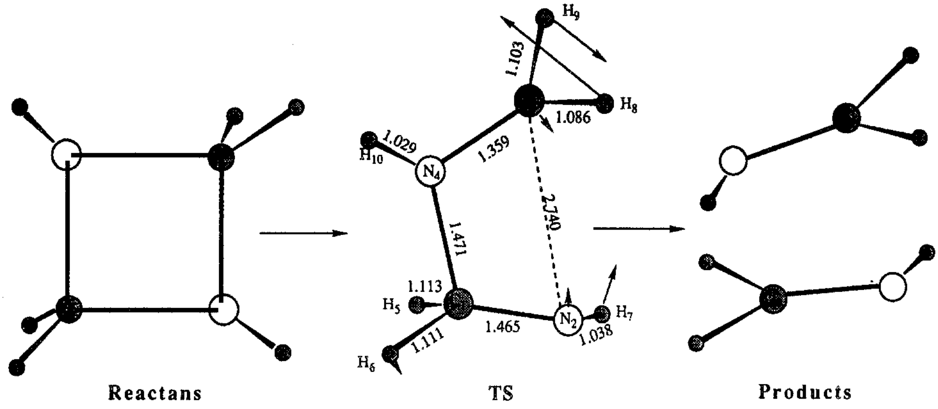

$H_{10}N_4C_1 = 128.8$
$N_4C_1N_2 = 102.3$
$C_1N_2C_3 = 73.2$
$H_5C_1N_2 = 119.5$
$H_6C_1N_2 = 109.3$
$H_7N_2C_1 = 106.9$
$H_9C_3N_2 = 152.8$
$H_8C_3N_2 = 70.1$

$C_1N_2C_3N_4 = -6.9$
$H_7N_2C_1N_4 = 107.1$
$H_{10}N_4C_1H_5 = -48.8$
$H_6C_1N_2C_3 = 111.3$
$H_8C_3N_2C_1 = -128.4$
$H_9C_3N_2H_7 = 20.2$
$H_5C_1N_2C = -125.0$

Fig. 1. Reactants, transition states and products structures of 1,3-diazacyclobutane decomposition reaction. For the TS are reported normal vibrational modes other than some significant geometrical parameters (distance are in Å, valence and torsional angles in degrees)

because it is a symmetry-forbidden process. Previous *ab initio* computations [33, 34] employing different basis sets and correlation treatments have been performed by choosing the angle between the center of the square and the N–C bond as a reaction coordinate and imposing symmetry restrictions.

In our study the transition state search has been done at the nonlocal level without any symmetry constraints using a (621/411/1*) orbital basis set (OBS) for carbon and nitrogen and (41) for hydrogen. The corresponding ABS are (4,3; 4,3) for C and N and (3, 1; 3, 1) for H atoms. The transition state found is completely different from that obtained at the *ab initio* level. Our structure (see Fig. 1) indicates that the two N–C bonds are not broken simultaneously, giving rise to an asymmetric transition state. From an analysis of the transition state normal vibrational modes it is evident that in the ring opening process, N_2–C_3 bond cleavage is more pronounced than that of N_4–C_1 and is accompanied by a $C_3H_8H_9$ group twisting plus a N_4–C_3 bond shortening. Table 4 summarizes the equilibrium geometries obtained for reactants and products and Fig. 1 shows the most significant values of transition state geometrical parameters. In Table 5 our energetic parameters are collected together with those previously found at different levels of theory [33, 34].

All methods predict 1,3-diazacyclobutane to be the more stable structure, but significative differences appear in the ΔE value between products and reactants. We find a ΔE value of 5.4 kcal/mol. Previous single point density functional computations [33, 34], performed by using geometries optimized at different *ab initio* and semiempirical methods and neglect of nonlocal corrections, give values that are

Table 4. Geometrical parameters for the 1,3-diazacyclobutane and its decomposition products. Distance are in Å and angles in degrees

Molecule	R_{N-C}	R_{C-H}	R_{N-H}	HNC	HCN
$C_2H_4NH_2$	1.501	1.117	1.037	110.3	114.2
CH_2NH	1.286	1.115	1.048	109.1	118.3
		1.122			125.8

Table 5. Activation energy (E_a) for the 1,3-diazacyclobutane decomposition and relative stability of the decomposition products (ΔE). Data are in kcal/mol. HF, MP4 and LDF data are taken from Refs. [33, 34]

Method	Geometry optimization	E_a	ΔE
NLSD	NLSD	37.6	5.4
HF/STO-3G	STO-3G	151.0	59.8
HF/3-21G*	3-21G	84.2	9.2
HF/6-21G*	3-21G	78.3	4.1
MP4/6-21G**	3-21G	76.0	2.3
LDF/DN[a]	AM1	66.8	19.2
LDF/DN[a]	STO-3G	67.9	20.7
LDF/DN[a]	3-21G	68.5	24.7
LDF/DND[b]	3-21G	68.4	25.8

[a] DN = double numerical

[b] DND = double numerical plus polarization function

much larger. The activation energy (E_a) that we obtain is 37.6 kcal/mol. Again we note that all other methods overestimate E_a. In this case the overestimation is probably due to the different shape of the transition state rather than to the lack of nonlocal corrections and to the use of "guest" geometries in the case of LDF calculations.

4. Conclusions

In this paper we have reported two examples of reaction energy profiles studied using density functional theory with transition states located using a step-by step uphill walking procedure along the minimum energy path followed by a refining procedure. For the isomerization reactions our results compare well with previous studies while an alternative picture of the transition state for the ring opening of 1,3-diazacyclobutane is proposed. Further work is in progress in order to extend the reliability of density functional potential energy surfaces and to test our TS algorithm for other reactions including systems containing transition metals.

Acknowledgements. The financial aid of CNR (Comitato Nazionale Scienza e Tecnologia Informazione, Comitato Nazionale Scienze Chimiche and Progetto Finalizzato Chimica Fine 2) and MURST is highly appreciated.

References

1. Fan L, Ziegler T (1990) J Chem Phys 92:3645
2. Fan L, Ziegler T (1992) J Am Chem Soc 114:10890
3. Amsterdam Density Functional System (ADF), Department of Theoretical Chemsitry, Vrije Universiteit, Amsterdam, The Netherlands. Baerends EJ, Ros P (1978) Int J Quantum Chem S12: 169
4. Stanton RV, Merz KM Jr (1994) J Chem Phys 100:434
5. Abashkin Y, Russo N (1994) J Chem Phys 100:4477
6. St-Amant A (1992) PhD thesis, Université de Montréal
7. Abashkin Y, Russo N, Toscano M (1994) Int J Quantum Chem 52:695
8. McIver JW, Komornicki A (1972) J Am Chem Soc 94:2625
9. Bell S, Crighton JS (1984) J Chem Phys 80: 2464 and references therein
10. Banerjee A, Adams N, Simons J, Shepard R (1985) J Phys Chem 89:52
11. Cummins PL, Gready JE (1989) J Comput Chem 10:939
12. Halgren TA, Lipscomb WN (1977) Chem Phys Lett 49:225
13. Rothman MJ, Lohr LL (1980) Chem Phys Lett 70:405
14. Muller K, Brown LD (1979) Theoret Chim Acta 55:75
15. Dewar MJS, Healy EF, Stewart JJP (1983) J Chem Soc 87:2745
16. Cerjan CJ, Miller WH (1981) J Chem Phys 75:2800
17. Simons J, Jorgensen P, Taylor H, Ozment J (1983) J Phys Chem 87:2745
18. Jorgensen P, Jensen HJA, Helgaker T (1988) Theoret Chim Acta 73:55
19. Vosko SH, Wilk L, Nusaiz M (1980) Can. J. Phys. 58:1200
20. Pezdew JP, Wang Y (1986) Phys Rev B33:8800; Pezdew JP (1986) Phys. Rev. B33:8822
21. Broyden CC (1970) J Inst Math Appl 6:76
22. Fletcher R (1970) Comput J 13:317
23. Goldfarb D (1970) Math Comput 24:23
24. Shanno DF (1970) Math Comput 24:647
25. Callomon JH, Hirota E, Kuchitsu K, Lafferty WJ, Maki AG, Pote CS (1976) In: Hellewege KH, Hellewege AM (eds) Structure data on free polyatomic molecules, Landolt-Bornstein, New Series, Group II, vol 7. Springer, Berlin
26. Hehre WJ, Radom L, Schleyer PvR Pople JA (1986) In: *Ab initio* molecular orbital theory. Wiley, New York and references therein.
27. Kamiya K, Morokuma K (1991) J Chem Phys 94:7287
28. Goddard JD, Yamaguchi Y, Schaefer III, HF (1981) J Chem Phys 75:3459
29. Deng L, Ziegler T, Fan L (1993) J Chem Phys 99:3823
30. Becke AD (1988) Phys Rev A38:3098
31. Pau CF, Hehre WJ (1982) J Phys Chem 86:1252
32. Saxon RP, Yoshimine M (1989) J Phys Chem 93:3130
33. Grodzicki M, Seminario JM, Politzer P (1990) Theoret Chim Acta 77:359
34. Grodzicki M, Seminario JM, Politzer P (1991) J Chem Phys 94:1668